

Strain-Based Design and Assessment in Critical Areas of Pipeline Systems with Realistic Anomalies

Appendix C: Curved Wide Plate Testing

Contract No. DTPH56-14-H-00003

Prepared for

US Department of Transportation
Pipeline and Hazardous Materials Safety Administration
Office of Pipeline Safety

Prepared by

Timothy Weeks

NIST

July 10, 2017

Notice

This project was funded by the Department of Transportation, Pipeline and Hazardous Materials Safety Administration under the Pipeline Safety Research and Development Program. The views and conclusions contained in this document are those of the authors and should not be interpreted as representing the official policies, either expressed or implied, of the Pipeline and Hazardous Materials Safety Administration, or the U.S. Government.

This work is the contribution of an agency of the U.S. government, and is not subject to copyright.

Acknowledgements

NIST gratefully acknowledges the technical contribution of Ross Rentz for his participation in every aspect of the CWP test program.

Table of Contents

Notice	i
Acknowledgements	ii
Nomenclature	C-1
Abbreviations	C-1
Organizations	C-1
Appendix C – Curved Wide Plate Testing	C-2
C.1 Curved Wide Plate (CWP) Specimen Sectioning	C-2
C.2 Notch Location Layout	C-7
C.3 Specimen Notching	C-8
C.4 Specimen Assembly	C-16
C.5 Test Equipment, Instrumentation and Measurements	C-19
C.6 Test Procedure	C-24
C.7 Post-Test Data Reduction	C-25
C.8 Post-Test Surface Notch Mouth Opening Photographs	C-30
C.9 Post-Test Fracture Surface Photographs	C-31

Nomenclature

Abbreviations

BM	Pipe base metal
CMOD	Crack mouth opening displacement
CTOD	Crack tip opening displacement
CTOD _A	Apparent CTOD toughness
CTOD _F	CTOD driving force
CTOD _R	CTOD resistance
CWP	Curved wide plate
DIC	Digital image correlation
HAZ	Heat affected zone
ID	Inside diameter
LVDT	Linear variable displacement transducer
OD	Outside diameter
SE(T)	Single edge notch tension
UTS	Ultimate tensile strength
WT	Wall thickness

Organizations

CRES	Center for Reliable Energy Systems
NIST	National Institute of Standards and Technology

Appendix C - Curved Wide Plate Testing

C.1 Curved Wide Plate (CWP) Specimen Sectioning

The CWP test specimens were sectioned from the two welded pipes in several steps to include plasma cutting of longitudinal strips followed by waterjet cutting the net specimen shape. The 12 o'clock reference is defined by an axial line that bisects the girth weld between the seam welds of each pipe section. The offset between seam welds was not the same between the two pipes. This is shown in the annotated photograph in Figure C1. The sectioning plan was designed to maximize the coincidence between circumferential locations of the CWP specimens. This is shown by the axial centerlines drawn within the CWP specimens in Figure C2.

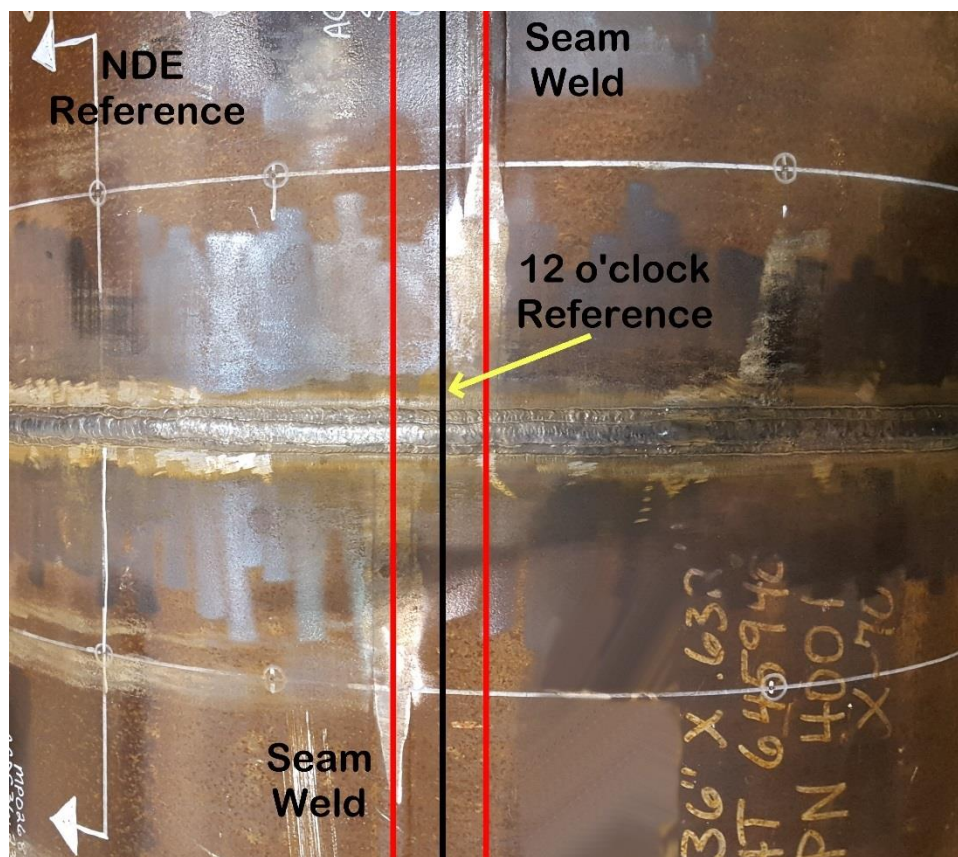


Figure C1 Annotated photograph of a pipe section girth weld with lines (red) aligned with each seam and the 12 o'clock reference line (black) used throughout the test program. The SERIMAX TOFD Weld Inspection Report used a different reference and direction as indicated in the photograph.

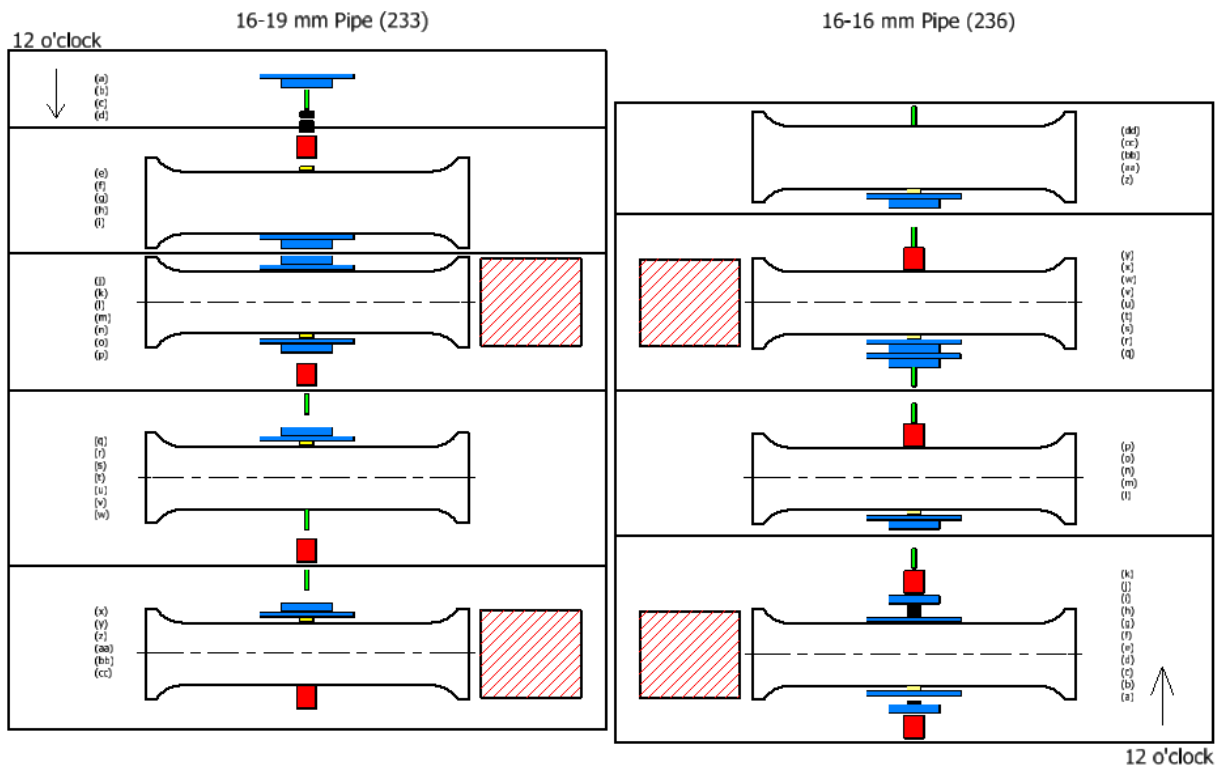


Figure C2 Schematic diagram indicating the location of CWP and small scale test sections. The 12 o'clock references are opposite in this view for the purpose of measurements and to show location coincidence between CWP specimens sectioned from the two pipes.

The reference letters shown in Figure C2 are described with small scale specimen identifiers shown in Table C1 and Table C2 for the 16 mm – 19 mm WT welded pipe (Weld 233 (Weld-2)) and the 16 mm – 16 mm WT welded pipe (Weld 236 (Weld-1)) respectively.

Table C1 Specimen sectioning legend for the 16 mm – 19 mm WT welded pipe (Weld 233 (Weld-2)).

Reference	Specimen ID	Reference	Specimen ID	Reference	Specimen ID
a	SET-1	k	SET-3	u	CWP-3
b	CTOD-1	l	CWP-2	v	AWMT-3
c	AWMT-1	m	Hardness-2	w	Charpy-3
d	NDE Indications	n	SET-4	x	AWMT-4
e	Charpy - 1	o	CTOD-4	y	CTOD-6
f	Hardness-1	p	Charpy-2	z	SET-6
g	CWP-1	q	AWMT-2	aa	Hardness-4
h	SET-2	r	CTOD-5	bb	CWP-4
i	CTOD-2	s	SET-5	cc	Charpy-4
j	CTOD-3	t	Hardness-3		

Table C2 Specimen sectioning legend for the 16 mm – 16 mm WT welded pipe (Weld 236 (Weld-1))

Reference	Specimen ID	Reference	Specimen ID	Reference	Specimen ID
a	Charpy-1	k	AWMT-1	u	SET-5
b	CTOD-1	l	CTOD-3	v	Hardness-3
c	NDE Indications	m	SET-3	w	CWP-3
d	SET-1	n	CWP-2	x	Charpy-4
e	Hardness-1	o	Charpy-3	y	AWMT-4
f	CWP-1	p	AWMT-2	z	CTOD-6
g	SET-2	q	AWMT-3	aa	SET-6
h	NDE Indications	r	CTOD-4	bb	Hardness-4
i	CTOD-2	s	SET-4	cc	CWP-4
j	Charpy-2	t	CTOD-5	dd	AWMT-5

The two welded pipe sections shown in Figure C3, were received at NIST directly from the welding vendor. Post-weld inspection reports were used to determine the locations of weld defects to be avoided for test specimens. The sectioning plan was designed to maximize the coincidence between circumferential locations of the CWP specimens. This is shown by the axial centerlines drawn within the CWP specimens shown in Figure C2. The sectioning plan was also optimized for the location and sectioning needs for small-scale specimens.



Figure C3 Photograph of the as-received girth welded pipe sections

The sectioning plan was transferred to the pipe sections and longitudinal strips were plasma cut from each pipe according to the drawings show in Figure C4 and Figure C5. These figures were also to inform the waterjet vendor of what they would expect and how to align the sections for waterjet cutting.

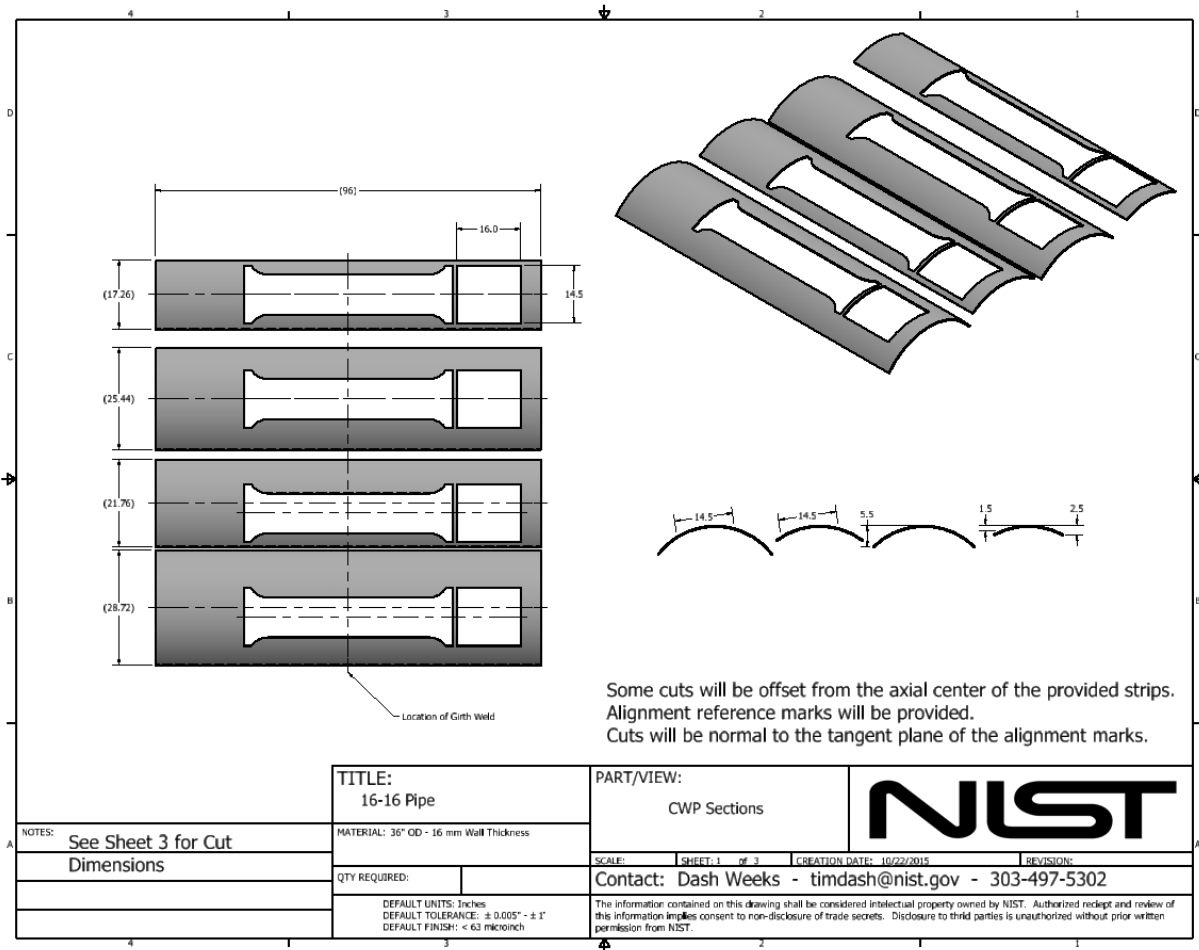


Figure C4 Machine drawing of longitudinal strip and CWP specimens sectioning plan for the 16 mm - 16 mm WT girth welded pipe (Weld 236 (Weld-1))

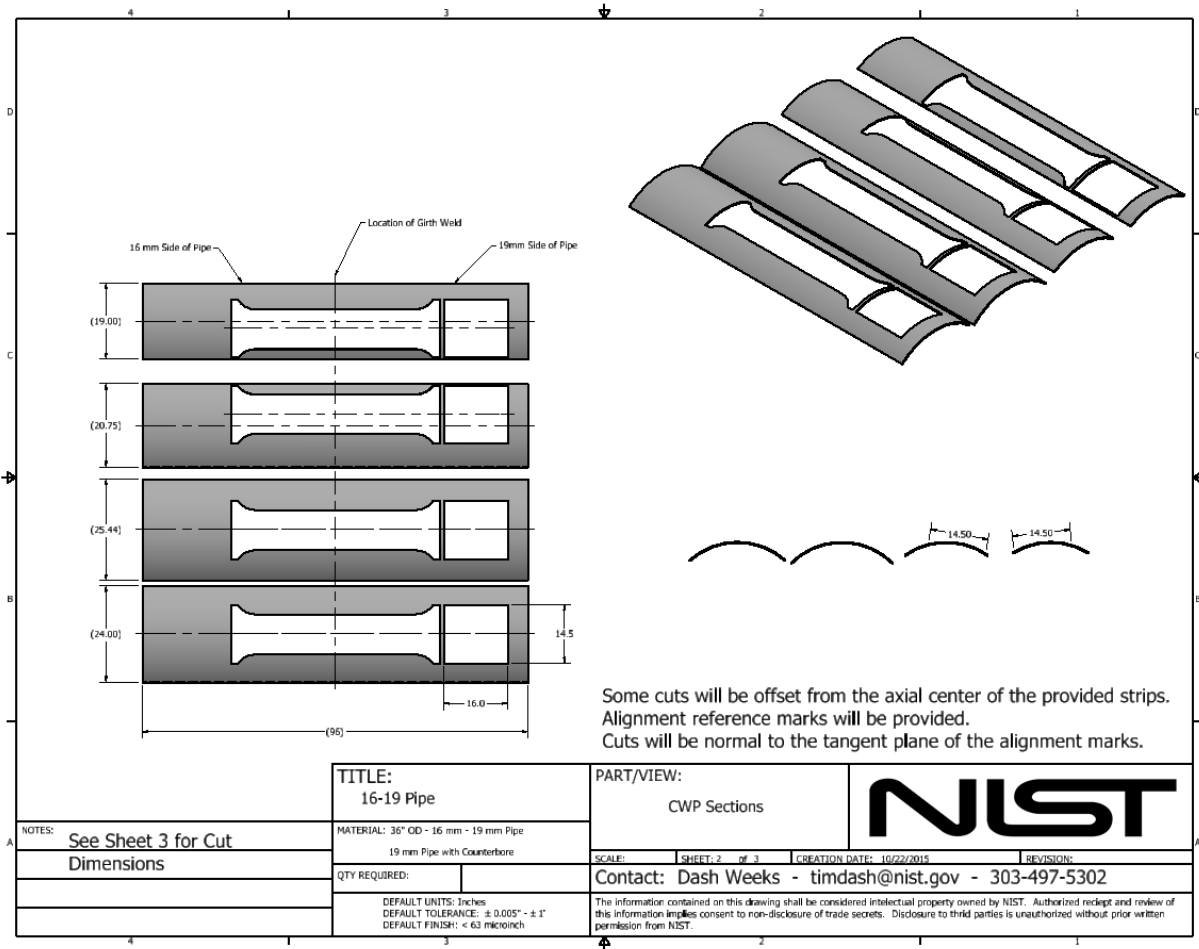


Figure C5 Machine drawing of longitudinal strip and CWP specimens sectioning plan for the 16 mm - 19 mm WT girth welded pipe (Weld 233 (Weld-2))

Each longitudinal strip included the CWP specimen and a panel used for base metal tension testing described in Appendix B. Only two of the four panels were sectioned for base metal testing and the remaining panels were retained for alternate tests if required.

Each of the CWP specimens were waterjet cut from the longitudinal strips and oriented to accommodate the difference in arc angles between the strip centerline and the specimen centerlines as shown in Figure C4 and Figure C5 for the two different pipes. The computer numerically controlled (CNC) waterjet was programmed for the same specimen profile for each pipe and is described in Figure C6. Strict controls on the waterjet speed ensured that the edges of each CWP specimen could be tested without additional machining.

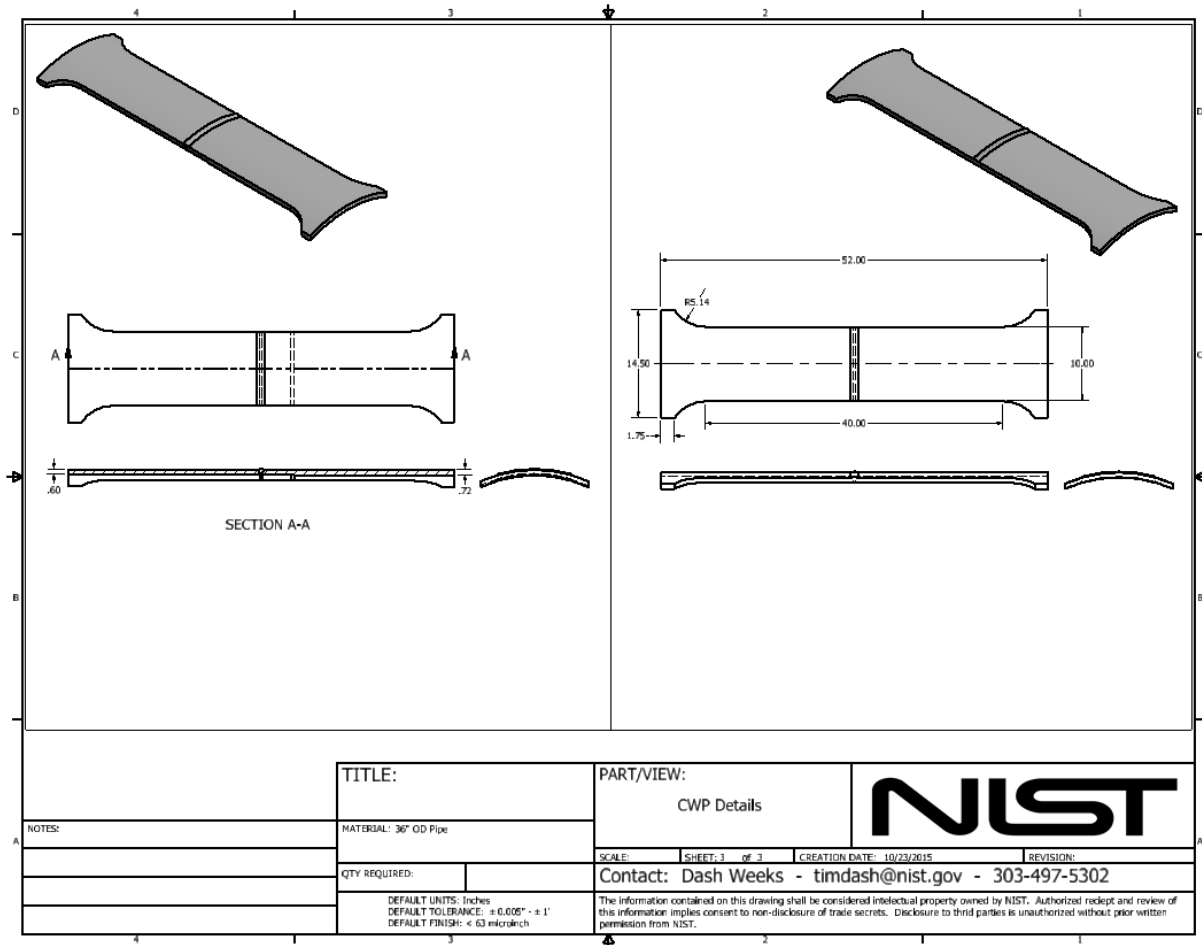


Figure C6 Machine drawing of CWP specimens for both pipes, 16 mm – 19 mm WT (Weld 233 (Weld-2)) on the left and 16 mm – 16 mm WT (Weld 236 (Weld-1)) on the right. The profiles are the same, however the change in thickness required a change in waterjet speed to maintain the same specimen edge quality.

C.2 Notch Location Layout

Once the CWP specimens were received at NIST from the waterjet vendor, each edge was polished and etched to reveal the location of the weld features. Each specimen was then scribed per the test matrix found in Table 3-18 of the main final report document.

Each specimen was scribed with lines indicating the 5mm depth of the notch. A photograph of this is shown in Figure C7. When necessary, the weld misalignment was accommodated by using the “low” side of the weld as the reference to measure from. Once the depth was determined then the axial placement of the notch was determined to either bi-sect the weld for WCL tests or located in the HAZ within 0.5 mm of the fusion line on each side of the specimen. This axial location was transferred to the ID surface of both edges and a scribe line was placed to

connect these locations. An axial alignment scribe was also placed on the ID surface of the specimens for the placement and orientation of the EDM notch.

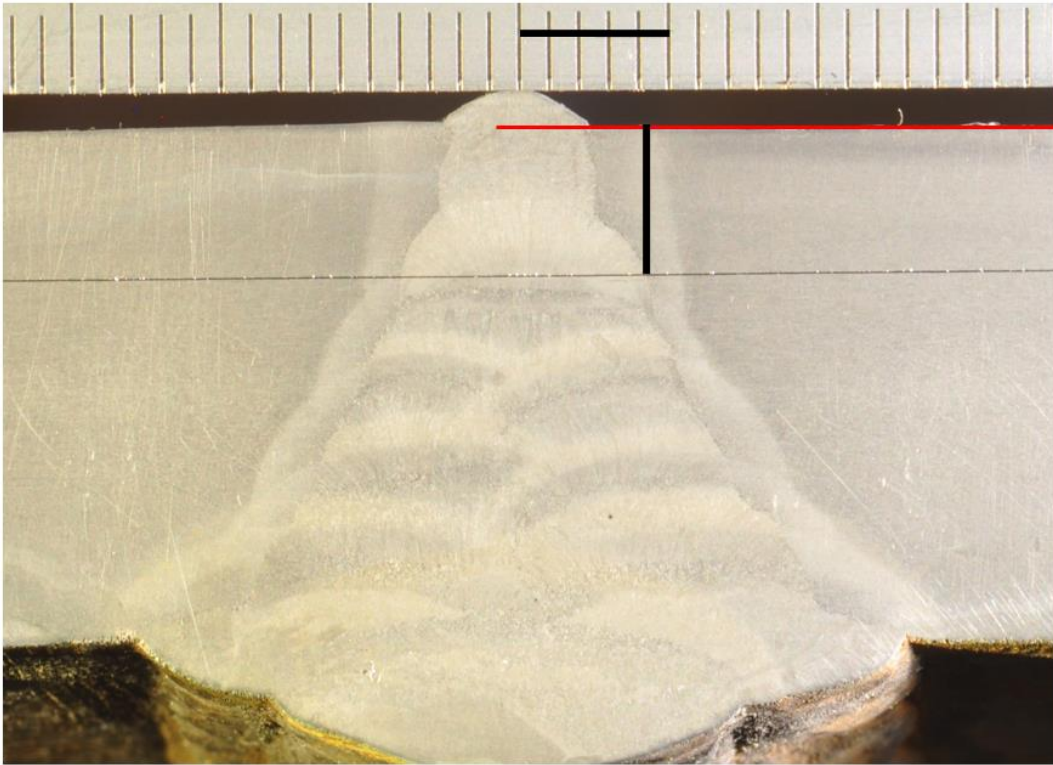


Figure C7 Photograph of a scribed CWP specimen edge to illustrate the measurement reference and location of the notch, the HAZ in this case for 236 CWP-1.

C.3 Specimen Notching

The specimens were shipped to the NIST machine shops in Gaithersburg, MD for the next steps in the specimen preparation. Each specimen end was beveled for welding, notched and welded to end tabs required for the test machine.

Prior to EDM notching, the weld cap was removed per the details found in Figure C8 and Figure C9 for the 16 mm – 16 mm (Weld 236 (Weld-1)) weld and 16 mm – 19 mm WT (Weld 233 (Weld-2)) weld respectively. Additional details for weld cap removal and notch placement can be found in Figure C10 for WCL notches and Figure C11 for HAZ notches, where these figures also describe how weld misalignment was accounted for in the cap removal process. In all cases the root weld cap was removed to be flush with the ID surface of the “low” side of the weld. This was done to accurately place the notches with consistent measurement references for the notch depth.

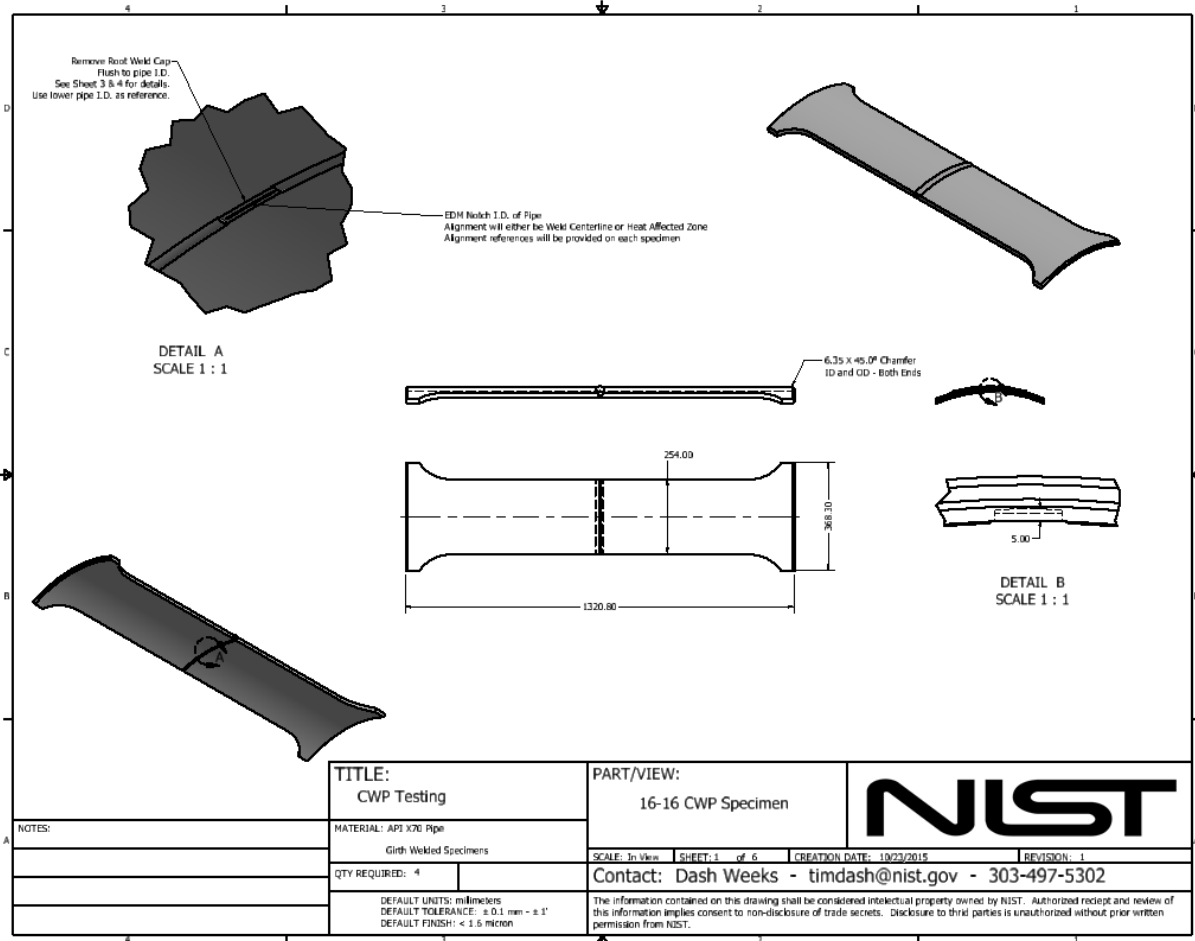


Figure C8 Machine drawing of notch details for CWP specimens extracted from the 16 mm to 18 mm WT girth welded pipe (Weld 236 (Weld-1))

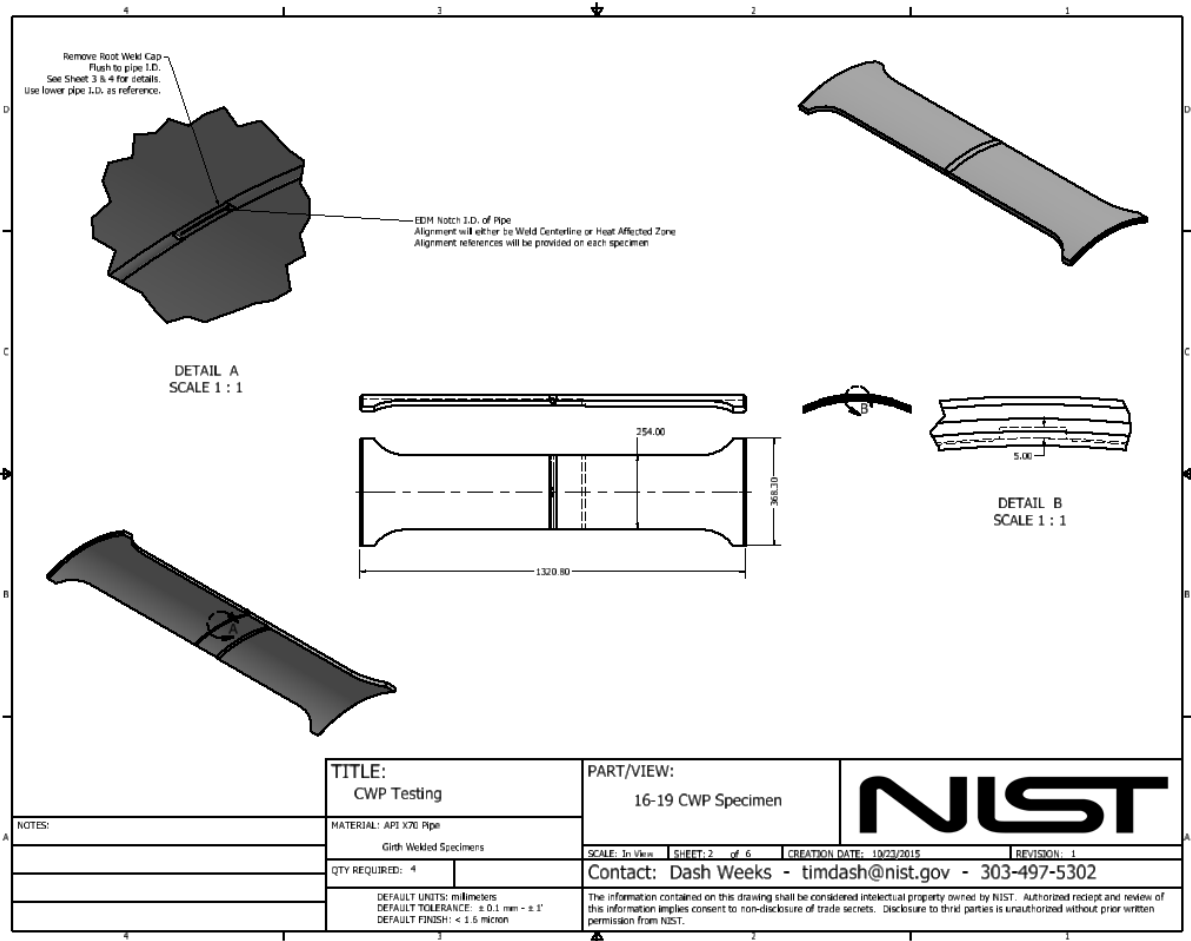


Figure C9 Machine drawing of notch details for CWP specimens extracted from the 16 mm to 19 mm WT girth welded pipe (Weld 233 (Weld-2))

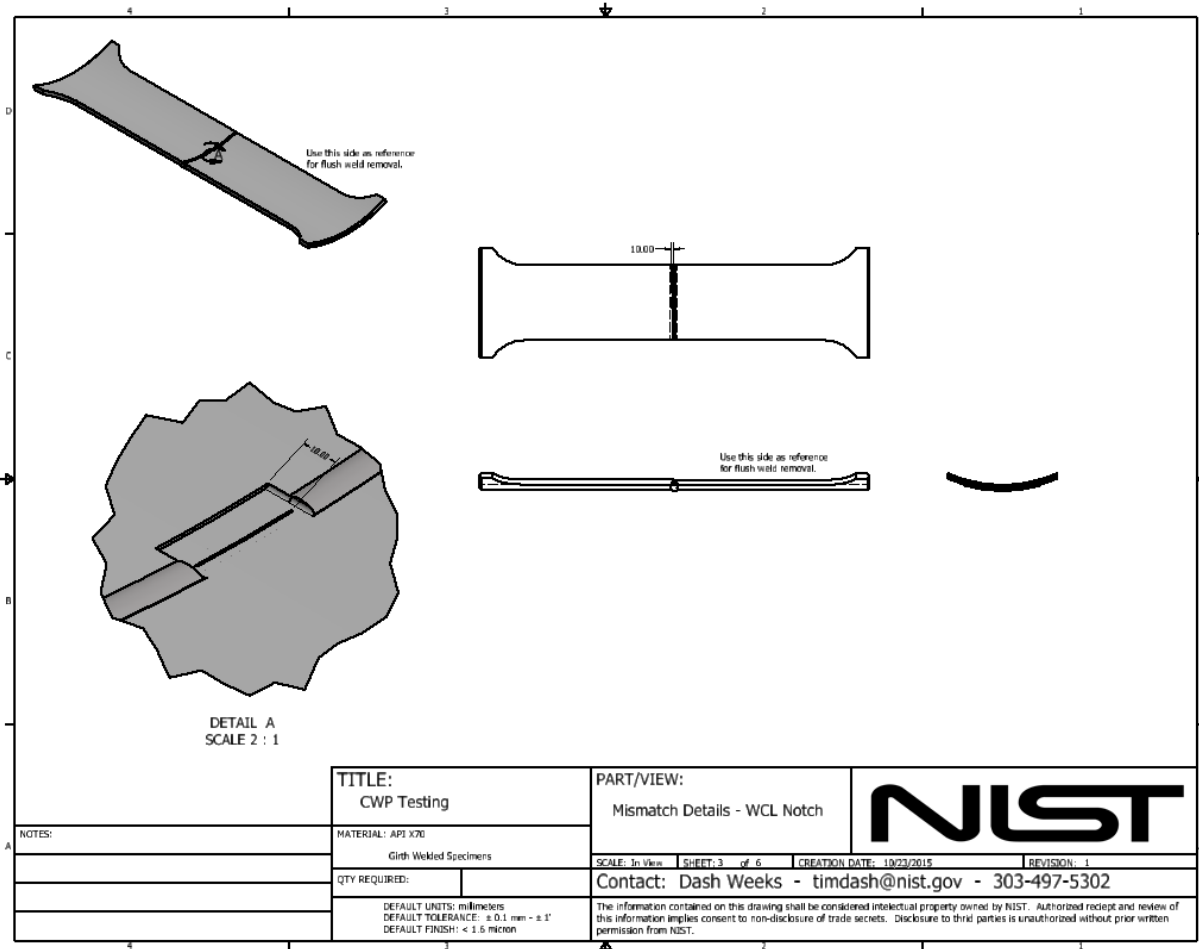


Figure C10 Machine drawing of notch details for CWP specimens highlighting the accommodation of weld misalignment and WCL notches

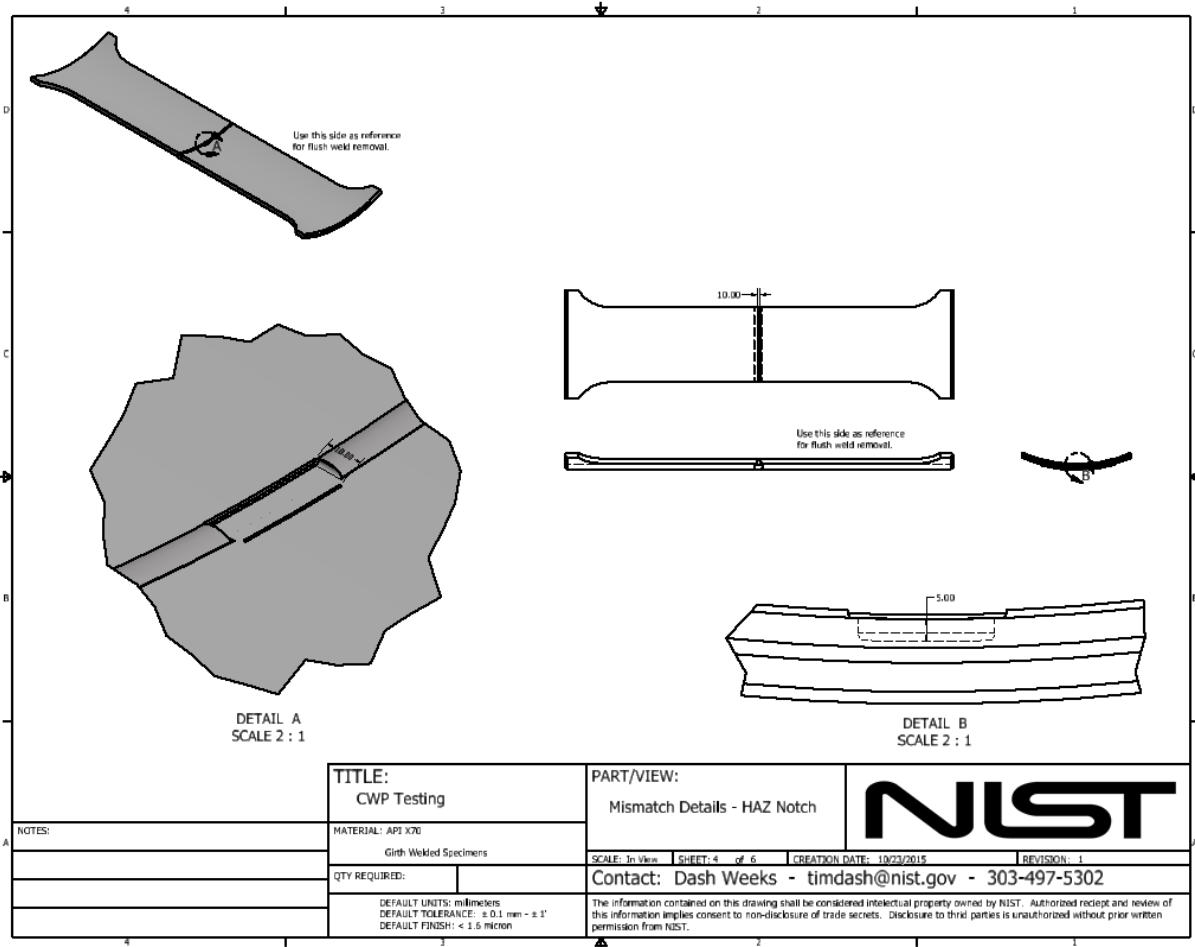


Figure C11 Machine drawing of notch details for CWP specimens highlighting the accommodation of weld misalignment and HAZ notches

The root weld cap was removed using the electrode design shown in Figure C12. The radius of the electrode was set to match the ID surface profile of each pipe and the root weld cap was removed flush with the ID surface of the “low” side of the weld.

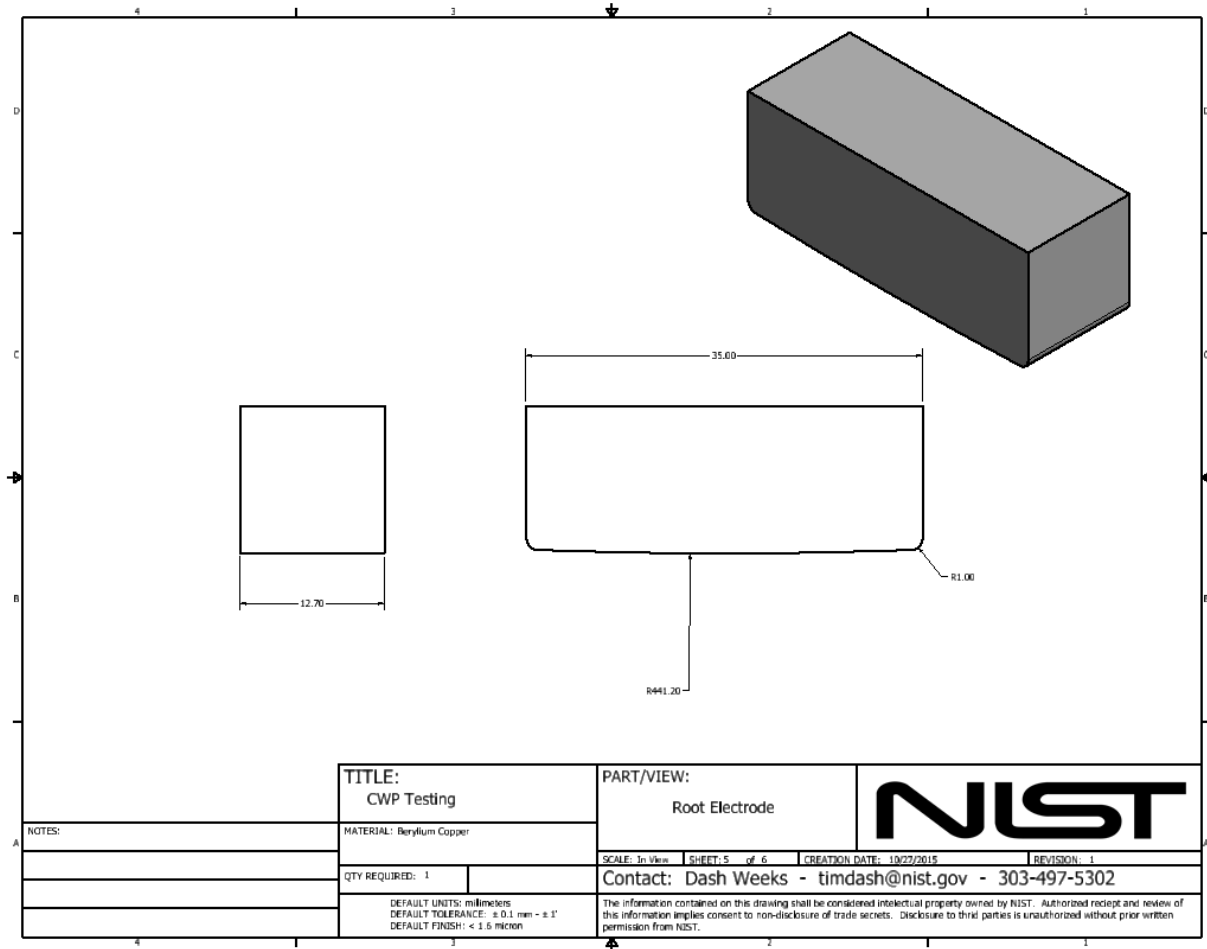


Figure C12 Machine drawing of the EDM electrode requirements for root weld cap removal

Each specimen was notched using the same electrode profile regardless of the notch location. The radius of the electrode was set to be concentric with the pipe and matches the ID radius plus 5 mm. The electrode design is shown in Figure C13. The step in the electrode served two purposes, first to accommodate the minimum gap needed for test instrumentation while maintaining a small notch root radius and to also maintain the stiffness of the electrode ensuring a planar notch. The root radius at the final notch depth was set to match the wire electrode used in SE(T) testing.

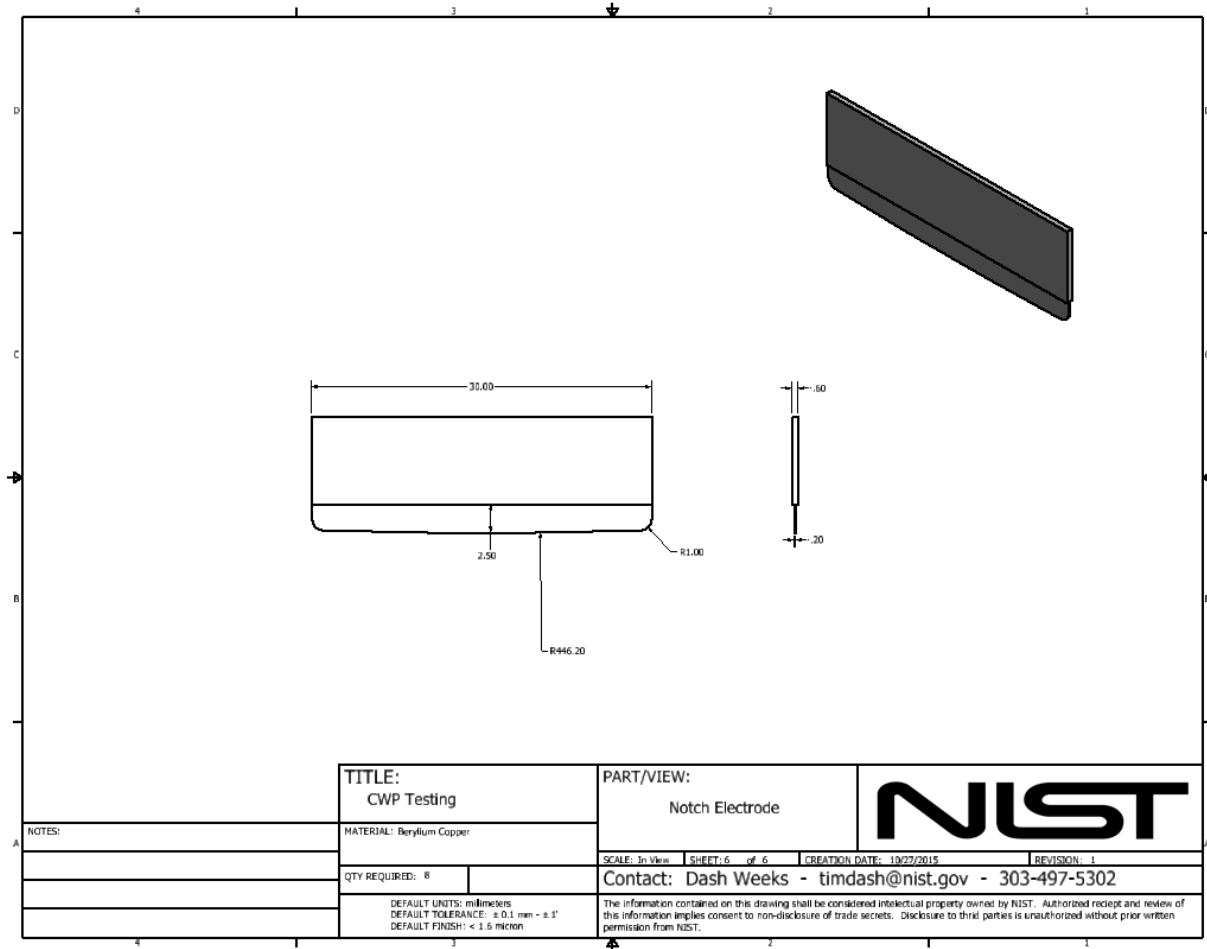
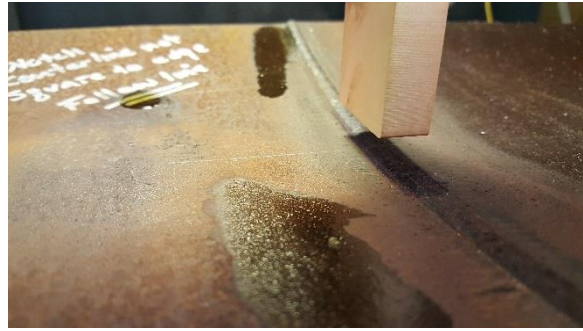


Figure C13 Machine drawing of the EDM electrode requirements for the notches placed in each specimen

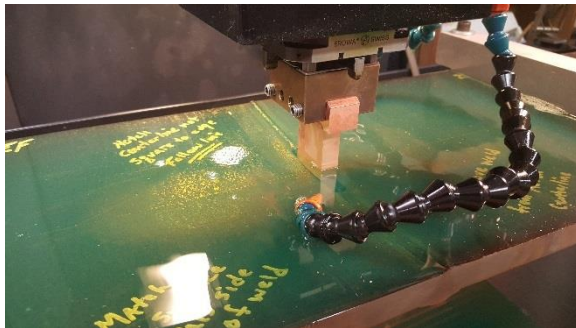
The EDM notching was conducted at the NIST machine shop in Gaithersburg, MD and the NIST principal investigator (PI) was present for setup and processing. Some photos of the process were taken and are shown in Figure C14.



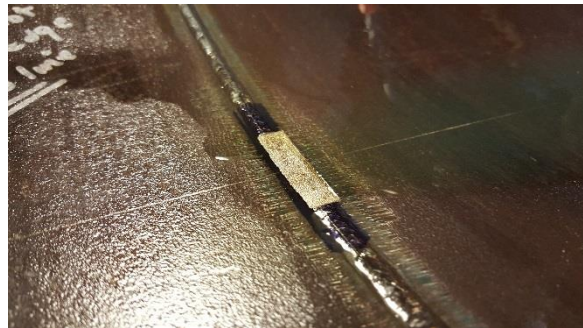
(a)



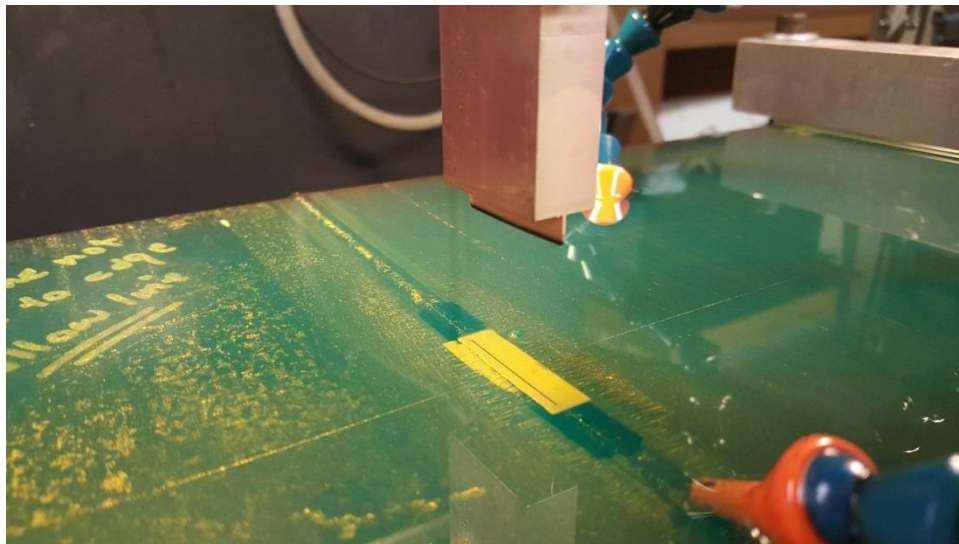
(b)



(c)



(d)



(e)

Figure C14 Photographs detailing the EDM process for each of the CWP notches. Photo (a) is of the initial setup and alignment with the root weld cap removal electrode. Photo (b) is a closer view of the root weld cap removal alignment step. Photo (c) was taken in process of root weld cap removal and photo (d) shows the removed root weld cap and is ready for notching. Photo (d) was taken with the notching electrode in view as well as the resulting notch.

C.4 Specimen Assembly

End tabs made of HSLA/HY100 steel were faced and prepared for welding to each specimen. The specimens were aligned within the grip end tabs to ensure that the axial load application was coincident with the centroid of the prismatic section of the specimen. The layout specifications are provided in Figure C15 and Figure C16 for the 16 mm – 16 mm WT welded specimens (Weld 236 (Weld-1)) and the 16 mm – 19 mm WT welded specimens (Weld 233 (Weld-2)) respectively. The welding procedure is detailed in Figure C-17. Details of the specimen end bevel can be found in Figure C8 and Figure C9 for each respective specimen.

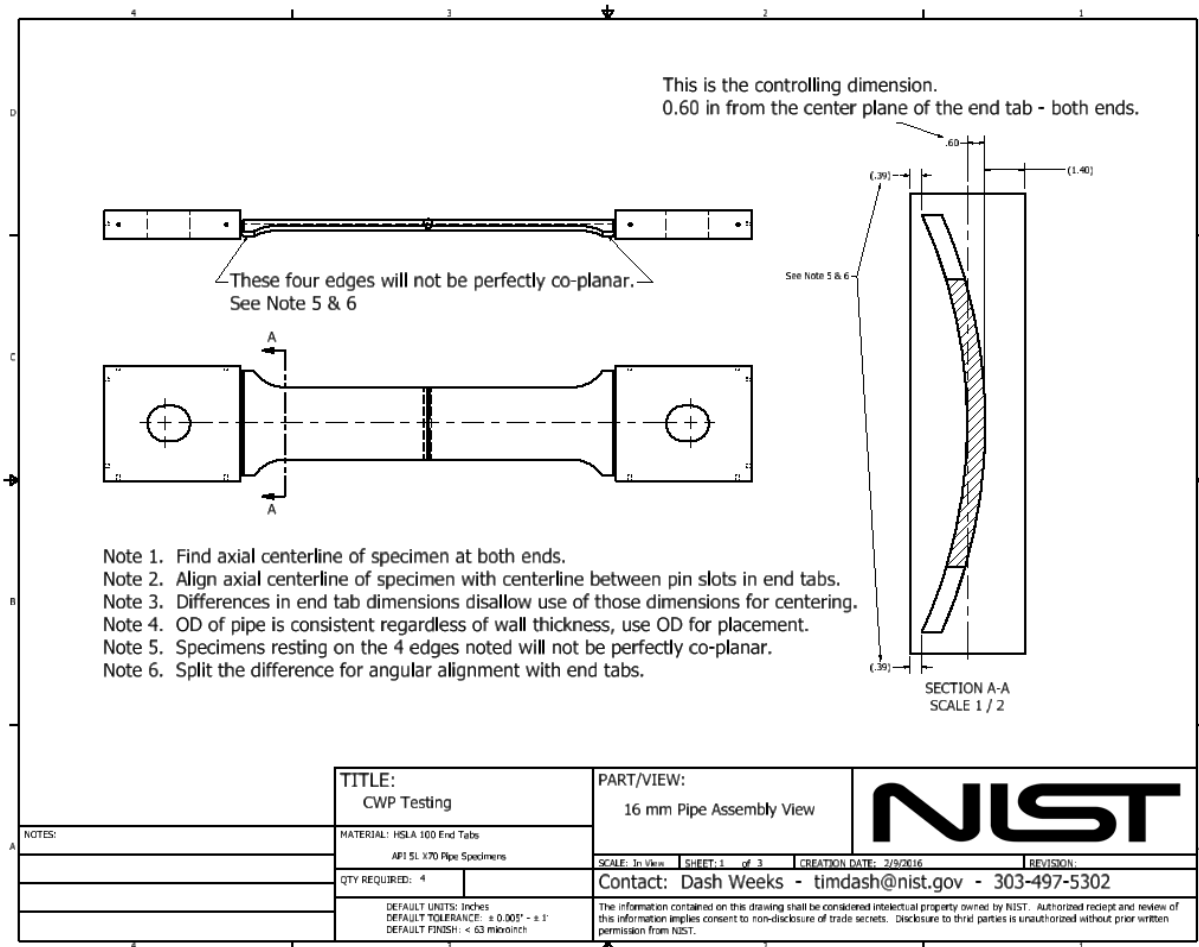


Figure C15 Machine drawing of the alignment requirements for the 16 mm – 16 mm WT welded CWP specimens (Weld 236 (Weld-1))

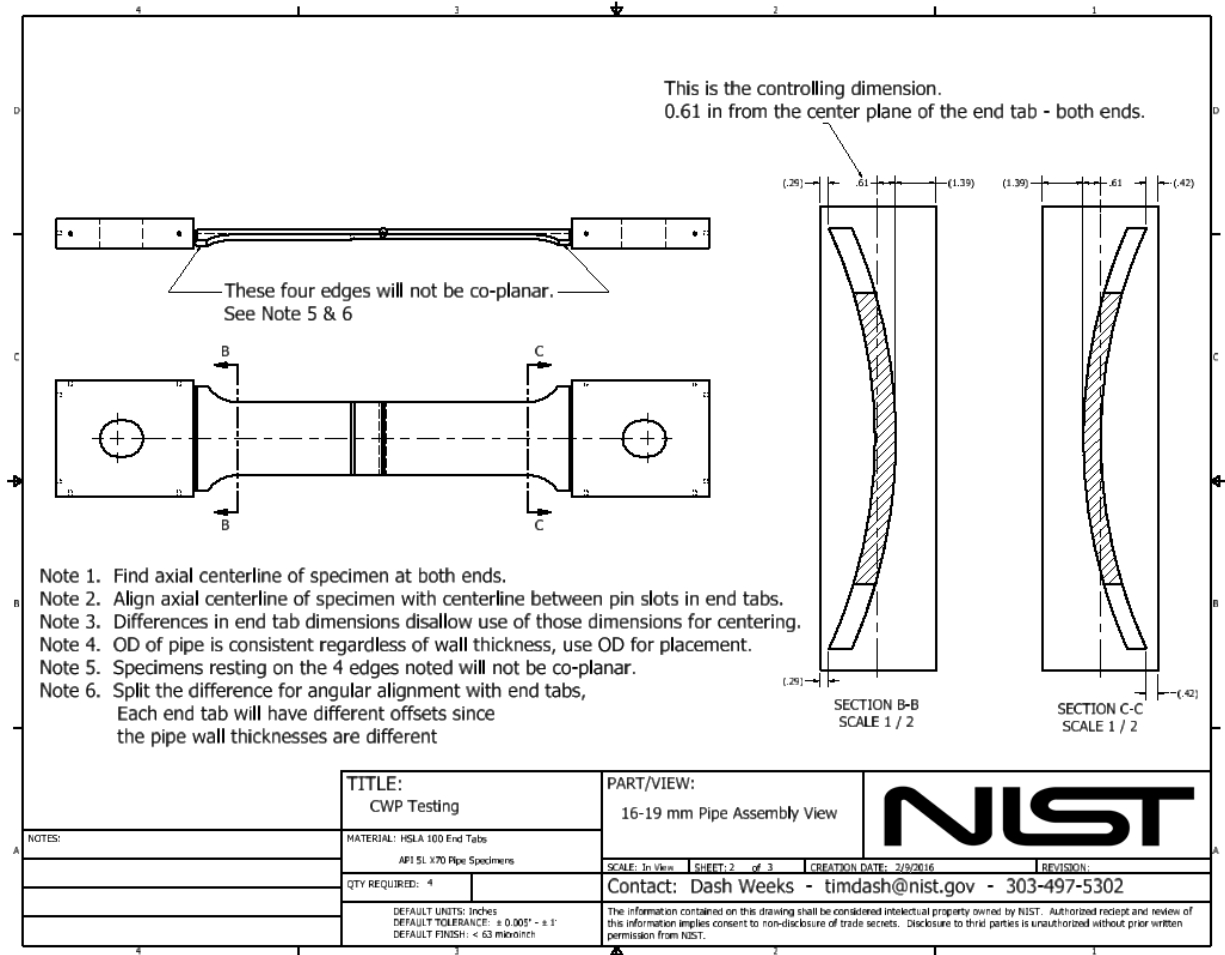


Figure C16 Machine drawing of the alignment requirements for the 16 mm – 19 mm WT welded CWP specimens (Weld 233 (Weld-2))

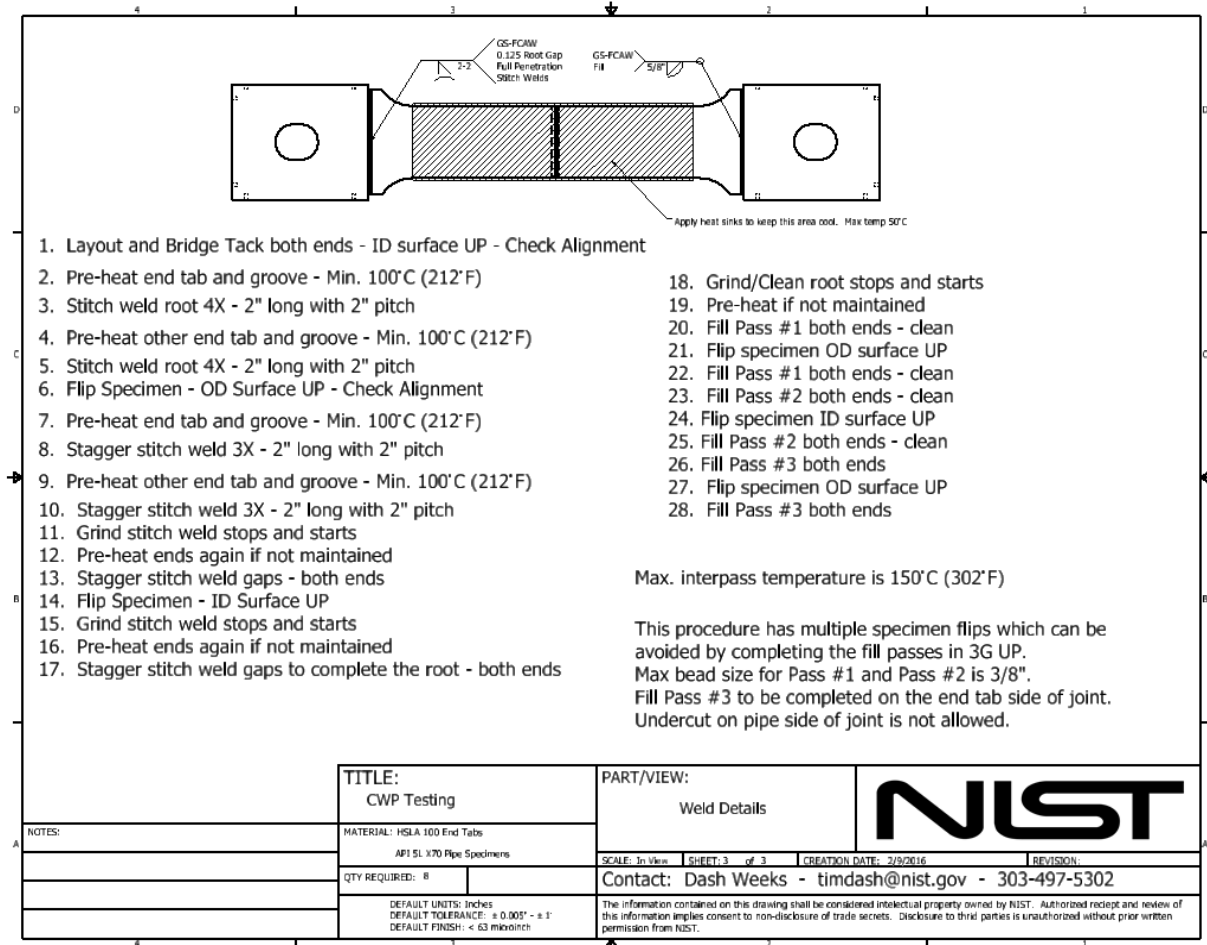


Figure C-17 Machine drawing of the end tab welding procedure for each CWP specimen

After the specimens were welded, they were shipped back to NIST in Boulder, CO for testing. The assembled specimens were shipped in specially designed steel shipping crates to eliminate the potential for specimen damage. Each crate could accommodate four specimens and an as-received crate is shown in Figure C18.



Figure C18 Photograph of four CWP specimens in their shipping crate as-received after notching and welding

C.5 Test Equipment, Instrumentation and Measurements

Load Frame

The load frame used at NIST for the CWP tests is a fixed upper-crosshead, bottom-actuated servo-hydraulic system. The frame and actuator are force-rated to 4.45 MN (1 Mlb) in tension. The actuator is capable of 147 mm (4.88 in) stroke. The upper crosshead is fixed only when a test is being conducted. The upper crosshead height (distance between grips) can be adjusted by the screw-driven lifts. The large force capacity and physical dimensions of a frame such as this is required for testing specimens of this scale.

Force Measurement

The force measurement is taken from the servo-hydraulic control system, which is connected to a quad bridge canister-style force transducer rated for 4.45 MN (1 Mlb). The load cell is connected to the fixed upper crosshead and is coaxial with the clevis grips and the load line of the specimen. For this test program, the servo-hydraulic controller was tuned for force control, as was necessary for preloading the specimen.

Stroke Measurement

The stroke (actuator displacement) measurement is taken from the servo-hydraulic control system, which is connected to an LVDT. The LVDT is directly connected to the bottom clevis

grip and gives an accurate record of actuator/grip position. The servo-hydraulic controller was also tuned for stroke control, as was necessary for the test profile.

Specimen Grips

Two clevis grips were machined from 4340 steel. The clevis grips are attached to the actuator and the load cell with a single centered threaded adapter. Each clevis accommodates a 127 mm (5 in) diameter hardened steel pin. The clevis grips allow much easier installation of a specimen for a specimen of this size. The clevis grips allow one degree of rotational freedom about the pins.

Strain Measurement

Each specimen was instrumented with six linear variable differential transformers (LVDTs) to capture remote pipe strain and cross weld strain. Four of the LVDTs were installed on the surfaces (ID and OD) of each half of the pipe (above and below the weld). These LVDTs were placed 76.2 mm (3 in) off-set from the axial centerline of the specimen and were in opposite sides from ID to OD. The nominal gauge length of the surface mounted LVDTs was 203.2 mm (8 in). The other two LVDTs were placed across the weld on opposing edges of each specimen. The nominal gauge length of these edge mounted LVDTs was 406.4 mm (16 in). All LVDTs were attached to the specimen by use of threaded studs. The threaded studs were installed onto each specimen by use of capacitive discharge (CD) welding, this method provided a secure mounting point without significant interaction with the specimen strain response. The exact gauge length between mounting studs was measured and recorded for each specimen. The layout and mounting configuration for the LVDTs can be found in Figure C19.

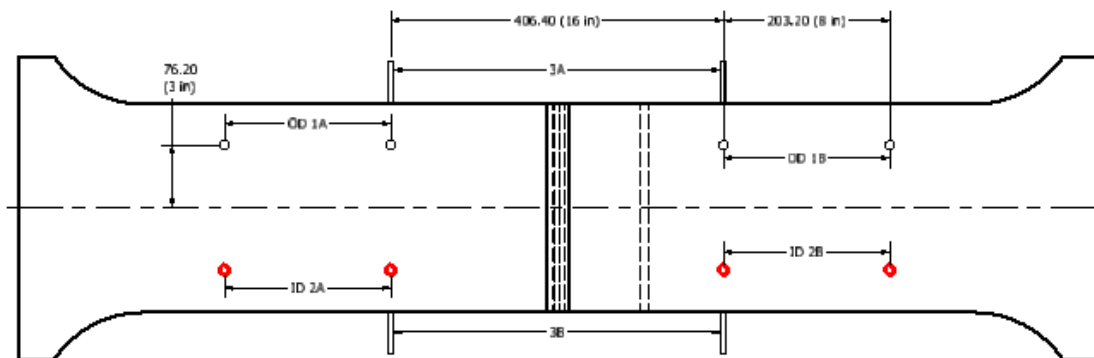


Figure C19 Illustration of the placement of the LVDTs mounted onto each of the CWP test specimens. This view is of the 16 mm – 19 mm WT pipe (Weld 233 (Weld-2)) but the layout was identical for all specimens.

In addition to the LVDTs, full field strain of the CWP specimens was captured by use of digital image correlation (DIC). This technique was used to verify the validity of the LVDT

data. The LVDT data is sensitive to strain distributions in the specimen that are a result of the test geometry. The DIC results are valuable to determine the strain distributions along and across the specimen.

The entire reduced section of each specimen (OD) was painted with a flat white epoxy paint followed by speckling. The specimens were speckled with a commercially available speckling kit that included a pattern roller with nominal dot sizes of 1.27 mm (0.05 in). The specimens were speckled with a black ink with a coverage of approximate ratio of white to black of 50 %. A commercial DIC system with 16 megapixel (MP) cameras was used for each test. The cameras were aligned vertically with the specimen axis. Both cameras were oriented in-plane with the specimen, with the first camera being located and aimed perpendicular to the plane and centered on the weld. The second camera was located and aimed at the specimen having an included angle of approximately 24 degrees. The entire specimen was illuminated with multiple sets of LED arrays. A photograph of a typical speckle pattern and system setup are shown in Figure C20.

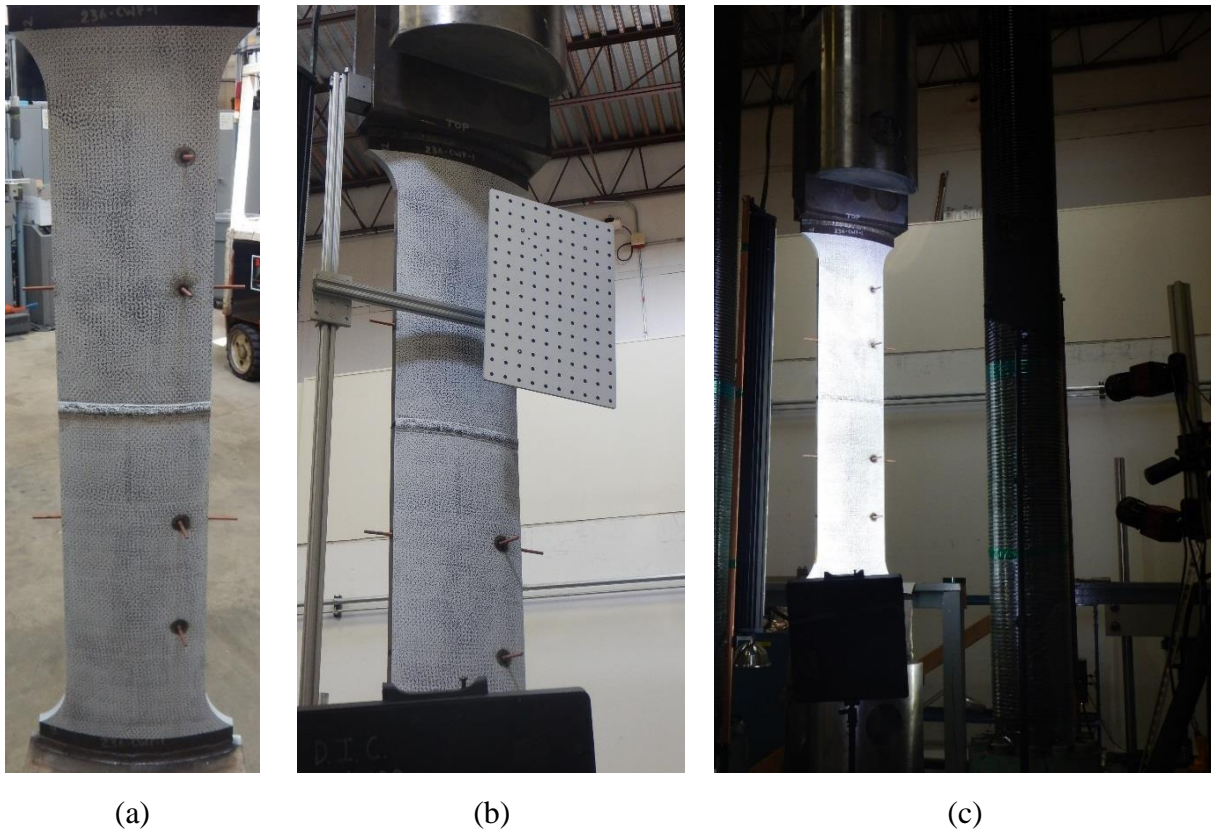


Figure C20 Photographs detailing the CWP specimen with DIC speckle pattern (a), calibration panel (b) and an illuminated specimen with cameras in view on the right (c). LVDTs are not yet installed on the threaded studs shown.

Crack Mouth Opening Displacement

A crack mouth opening displacement (CMOD) gauge was installed into the notch mouth of each CWP specimen and aligned with the axial centerline of the specimen. The CMOD gauge was a ring-type clip gauge with engagement teeth that fit inside the notch. The teeth were 0.6 mm (0.025 in) long. The CMOD gauge provided enough spring force to maintain the placement by friction but was also externally supported by use of a light spring steel clamp to keep the gauge inserted and square with the notch opening. A typical installation can be seen in the photograph shown in Figure C21.



Figure C21 Installation of the CMOD gauge and the spring clamp on the ID side of each CWP specimen

Calibrations

All instrumentation calibrations were performed per ASTM standards for the respective sensor types. Discreet calibration of DIC data is not yet standardized and in this case the system manufacturers calibration procedures were employed.

The LVDTs were calibrated end to end (sensor to data display) with a digital displacement calibrator. End to end calibrations were also performed on the CMOD gauges with a calibrated micrometer head according to ASTM E83.

The load cell and machine stroke LVDT were calibrated by the manufacturer on-site at NIST. The manufacturer maintains certification to conduct calibrations by the American Association for Laboratory Accreditation (A2LA). The manufacturer certified the accuracy of both the force transducer and the displacement transducer. A calibration block was manufactured from HSLA-100 plate steel to carry the full load of the frame capacity.

Pre-Test Specimen Measurements

Each of the specimens were measured by use of digital calipers to determine the chord width of the reduced section which is reported as the average of 5 points equally spaced from each end of the reduced gauge length. Each specimen thickness was also measured by use of digital micrometers equipped with spherical anvils. Eight thickness measurements were recorded for each specimen and the average thickness reported. Four thickness measurements were taken on each side of the specimen at approximately the same circumferential location as each of the LVDT mounting locations but were taken approximately 25 mm from the edge of the specimen (limited by the throat of the micrometers). For the 16 mm – 19 mm WT welded pipe (Weld 233 (Weld-2)) only the four measurements for each pipe section were used in the average, additionally the wall thickness of the counter bore in the 19 mm WT pipe were recorded in two locations on opposite edges of the specimen. Pre-test measurements for the 16 mm – 19 mm WT welded pipe (Weld 233 (Weld-2)) are presented in Table C3 and pre-test measurements for the 16 mm to 16 mm WT welded pipe (Weld 236 (Weld-1)) are presented in Table C4.

Table C3 Pre-test CWP specimen measurements for the 16 mm – 19 mm WT welded pipe (Weld 233 (Weld-2))

	233 CWP - 1	233 CWP - 2	233 CWP - 3	233 CWP - 4
Chord Specimen Width	254.25	254.21	254.10	254.29
Avg. Thickness (16 mm side)	16.85	16.89	16.92	16.82
Avg. Thickness (19 mm side)	19.82	19.88	19.83	19.84
C-Bore Thickness	15.73	15.67	15.65	15.72
LVDT Gauge Lengths				
1A	203.78	203.80	204.08	202.85
1B	203.89	203.07	203.32	202.23
2A	203.39	204.00	202.21	203.88
2B	204.20	203.52	204.29	203.79
3A	406.69	406.76	406.82	407.60
3B	406.66	405.63	405.12	408.88

Table C4 Pre-test CWP specimen measurements for the 16 mm – 16 mm WT welded pipe (Weld 236 (Weld-1))

	236 CWP - 1	236 CWP - 2	236 CWP - 3	236 CWP - 4
Chord Specimen Width	254.31	254.14	254.12	254.01
Avg. Thickness (16 mm side)	16.78	16.72	16.67	16.66
LVDT Gauge Lengths				
1A	202.87	203.08	204.28	203.37
1B	203.22	202.04	202.23	201.52
2A	203.82	202.65	203.64	204.31
2B	202.92	203.86	203.09	202.15
3A	406.83	406.45	406.81	407.16
3B	406.98	406.64	406.99	406.46

C.6 Test Procedure

All tests were carried out at ambient room temperature. The loading profile was programmed into the controller of the 4.45 MN (1 Mlbf) capacity servo-hydraulic test frame. The specimens were pre-loaded to approximately 5 kN (1.1 klbf). The loading profiles were separated into two sections, delineated approximately by the proportional limit. The goal was to complete eight unloading cycles before the net section stress reached approximately 50 % of the yield strength. Strap tensile test results for the 16 mm WT pipe (Weld 236 (Weld-1)) were used to set the machine programming; where the minimum yield strength (489 MPa) and minimum UTS (668 MPa) were used to achieve conservative programming limits. All loading, unloading and reloading commands were executed in displacement control at a rate of 6 mm/s. The loading program incorporated pre-programmed force limits to reverse the direction of the actuator. The unloading-reloading sequence prior to the proportional limit did not include a pause before unloading, whereas a three-second hold was programmed for the unloading-reloading sequences after the proportional limit.

The next unloading-reloading sequence was at an absolute load limit close to the net-section yield-load of the specimen based on reported yield strength. Due to the uncertain nature of the yielding event and low slope of the post-yield Force-CMOD data, the operator had the option of interrupting this loading cycle and manually initiating the next sequence if it appeared that the pre-programmed increment would have lost data in the transition.

The next section of the test involved unloading/reloading cycles in the plastic range, where the specimen was also unloaded and reloaded in displacement-control at a rate of 6 mm/s. The limits defining the start and stop of each unload/reload cycle used the machine stroke signal as a limit; a software loop was programmed to iterate the entire process. Beginning at the incremental load maximum (P_{Max}^i) of the current (i -th) loading segment, specimens were held in

displacement control for three seconds prior to unloading to a load 130 kN lower than P_{iMax} and then reloaded by 115 kN. Reloading the specimen by 115 kN ensured that the specimen was reloaded nominally elastically. Deformation was then continued until the machine stroke had increased by a relative 1.5 mm. When the stroke increment was reached, a new P_{iMax}^i value was defined (based on the load achieved at the end of the increment) and the loop was iterated. The machine stroke increment effectively defines the number of unloadings in the plastic portion of the test, with a goal of acquiring 20-30 unloading cycles prior to the specimen attaining a maximum in the applied force. The test continued past the maximum force and was terminated when any one of the following conditions were met; the CMOD reached 2.5 mm, the P_{iMax}^i was 80% of P_{Max} , the CMOD vs. machine stroke reached an asymptote or in some cases when the CMOD vs. machine stroke curve changed directions indicative of little or no change in CMOD with an increase in stroke.

C.7 Post-Test Data Reduction

Three data acquisition systems were employed for each specimen. The machine controller for the load frame was used accommodate the load, machine stroke and CMOD gauge. Each of these signals were also output from the controller to the other two data acquisition systems. A second instrumentation data acquisition system was a commercially available system capable of conditioning the six LVDTs while also accepting the output from the controller. This ensured that load, stroke, CMOD and the LVDTs signals were logged at the same acquisition rate of 20 Hz with common time stamps and thus avoiding the need to correlate signals from different systems post-test. The third data acquisition system was integral to the DIC system. The load, stroke and CMOD signals were logged with each photograph taken with the DIC system at a rate of 2 Hz. The DIC acquisition rate was lower than the other systems to maintain the full 16 MP images for full field strain measurement.

Signal Verification

The data fidelity between systems is the first verification step. Each data set from the three data acquisition systems were plotted on common axes to visually check that the systems were logging the same values regardless of data acquisition rate. This verification ensures that analysis of the raw data from any of the systems will produce the same result. The data for one of the specimens tested (233 CWP-2) were visually identical as shown in Figure C22. Since no single force-CMOD data pair were identical between data sets, five randomly selected values of CMOD were used to numerically compare the force value between systems. Furthermore, the CMOD values selected were linearly interpolated to ensure an exact comparison between systems. The force data associated with the selected CMOD value also required interpolation between adjacent points. Considering the machine controller data set as the standard, the other two systems were compared and the maximum difference found was 0.05 % of the load reading at the selected CMOD values. This is an order of magnitude better than the measurement uncertainty of both the force and CMOD data. These comparisons and results are typical and not all specimen data sets were quantitatively compared with this rigor.

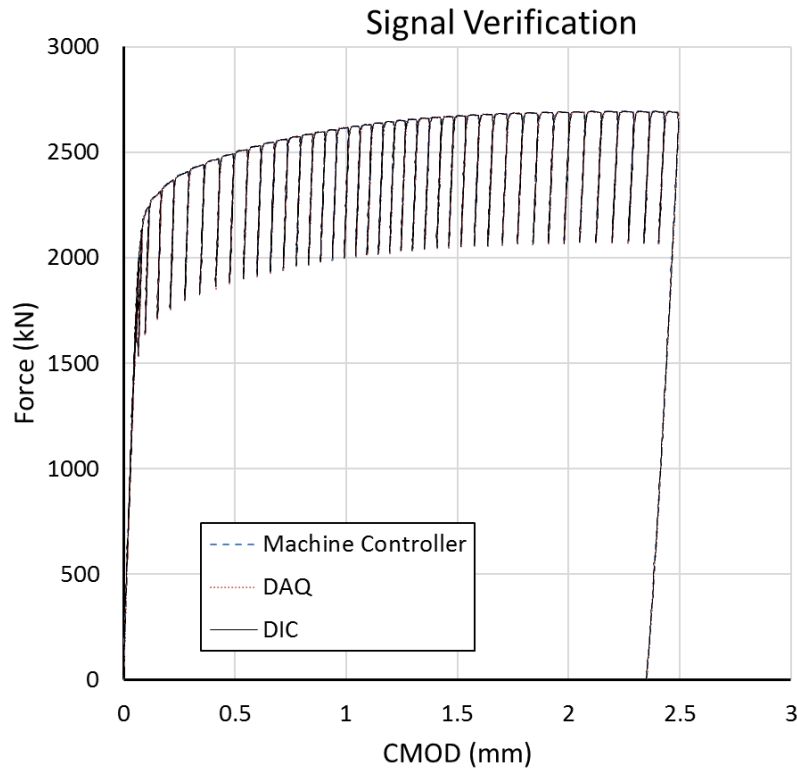


Figure C22 Force vs. CMOD data plotted from the machine controller, the external data acquisition system and the DIC data acquisition system for 233 CWP-2. Visually the data is identical and numerical comparisons between the data are less than 0.05 %.

Strain Verification

DIC strain data was verified by creating virtual extensometers that could then be compared to the LVDT data. This verification is necessary to ensure that the full field DIC strain data can be used quantitatively. This verification is unfortunately not an exact verification since vertical extensometers could not be created with exact LVDT mounting locations. The virtual extensometers were created with the same gauge length as the individual LVDT but were offset toward the axial centerline by approximately 19 mm (0.75 in) from the LVDT mounting studs. Future test programs will include targets on the ends of the mounting studs to make an exact verification. Despite the offset, all the virtual extensometers created matched within 2 % of the physical LVDT measurement. In all cases where there was a difference, it was due to localized strain in the pipe near the upper LVDT mounting stud and the difference increased with increasing localized strain. Figure C23 shows a plot of the force vs. the axial strain calculated from LVDT 1A and a virtual extensometer created in the DIC system. The inset photographs illustrate the strain gradients in the specimen. The color gradients scale with maximum strain and are therefore not equivalent between photos. The key feature to note is the high strain localization near the upper mounting stud of LVDT 1A which creates the offset difference in the comparison shown in the plot. Despite the obvious shift in strain later in the test, the difference shown is relatively small: LVDT 1A at 6.31 % strain as compared to the virtual extensometer

strain at 6.39 % strain. The result shown for the virtual extensometer is 1.4 % greater at that point. The data plot was truncated for illustration, however, the maximum strain difference at the end of the test for this specimen was 1.9 %.

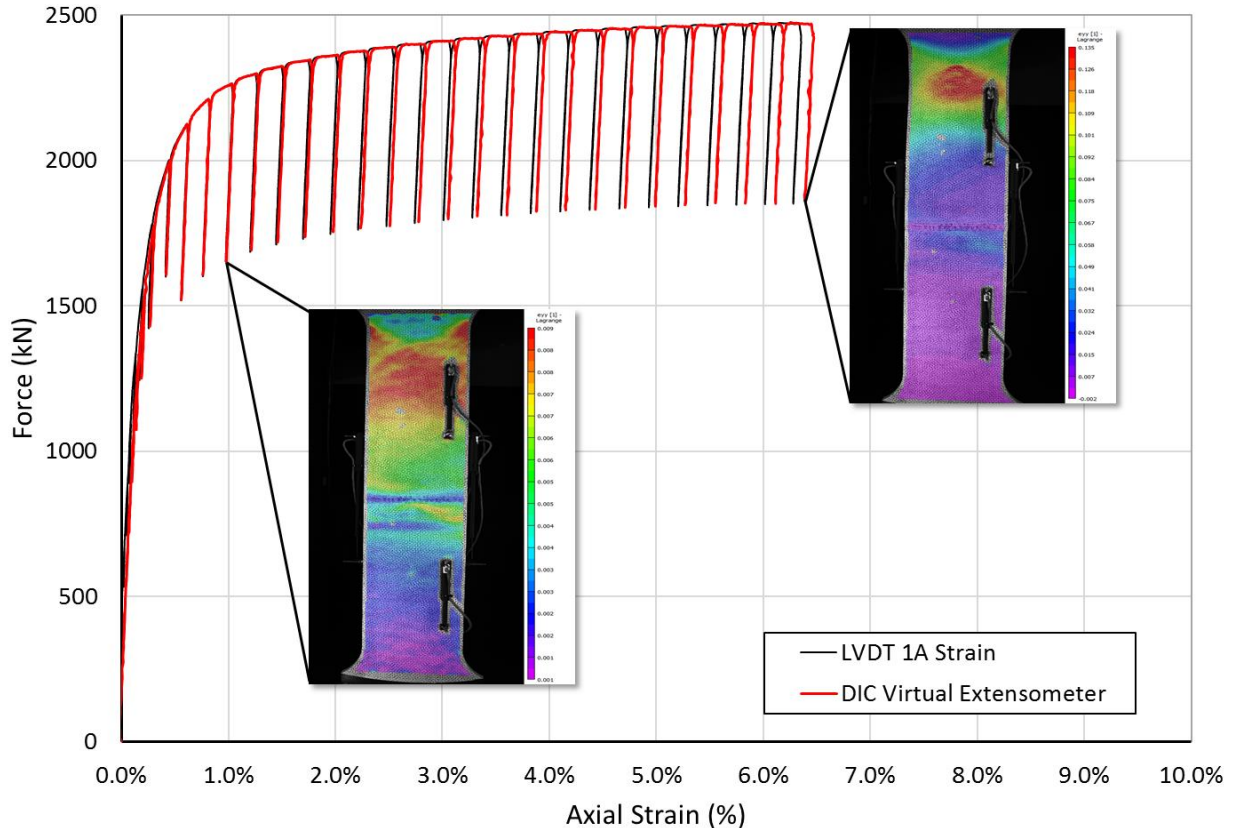


Figure C23 Plot of Force vs. Axial Strain for specimen 233 CWP-1, specifically comparing LVDT 1A with the virtual extensometer created in the DIC system. The inset photographs show the surface strain gradients near 1 % strain where the correlation is excellent and at ~6.3 % strain where the difference in DIC data is 1.4 % greater than LVDT 1A.

For each specimen, the average strains were calculated from OD and ID LVDTs. LVDT 1A and LVDT 2A were averaged for the upper pipe remote strain and similarly, LVDT 1B and LVDT 2B were averaged for the lower pipe remote strain. The final strain calculation was the cross-weld strain and was taken as the average of LVDT 3A and LVDT 3B.

Final Results

The reduced data in spreadsheets were provided to CRES for further analysis. The force vs. the remote strains in each pipe section as well as the cross-weld strains were plotted for each specimen. The typical results are shown in Figure C24. Additionally, the force vs. CMOD data were plotted for each specimen. The extreme over-matched weld properties caused considerable differences in the specimen response. Most of the specimens resulted in highly variable CMOD

response with very little crack extension. Furthermore, most of the specimens necked in the net section which caused a severe compression of the unloading cycles late in the test. In keeping with illustrating the response from 233 CWP-1, the plot of force vs. CMOD for this specimen is shown in Figure C25.

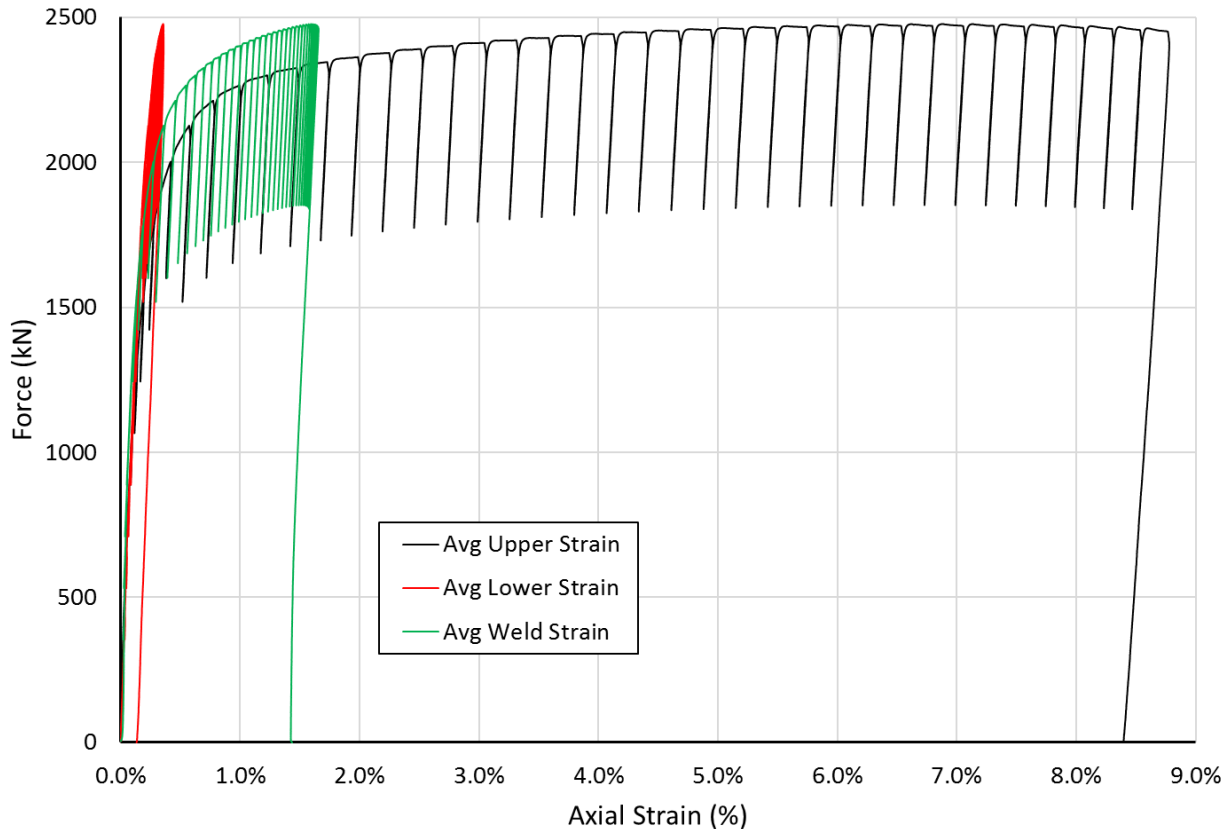


Figure C24 Plot of Force vs. Axial Strain for specimen 233 CWP-1, the three axial strains shown are the average upper, lower and cross-weld strains as calculated from the LVDTs.

Processed DIC images are used in this program to identify anomalous strain gradients in the test specimen and to capture the general strain response. Based on the quantitative comparisons already described, further DIC analysis was not necessary and added no additional value to the current objectives of the test program. Processed DIC images at the end of each test are presented in Figure C26.

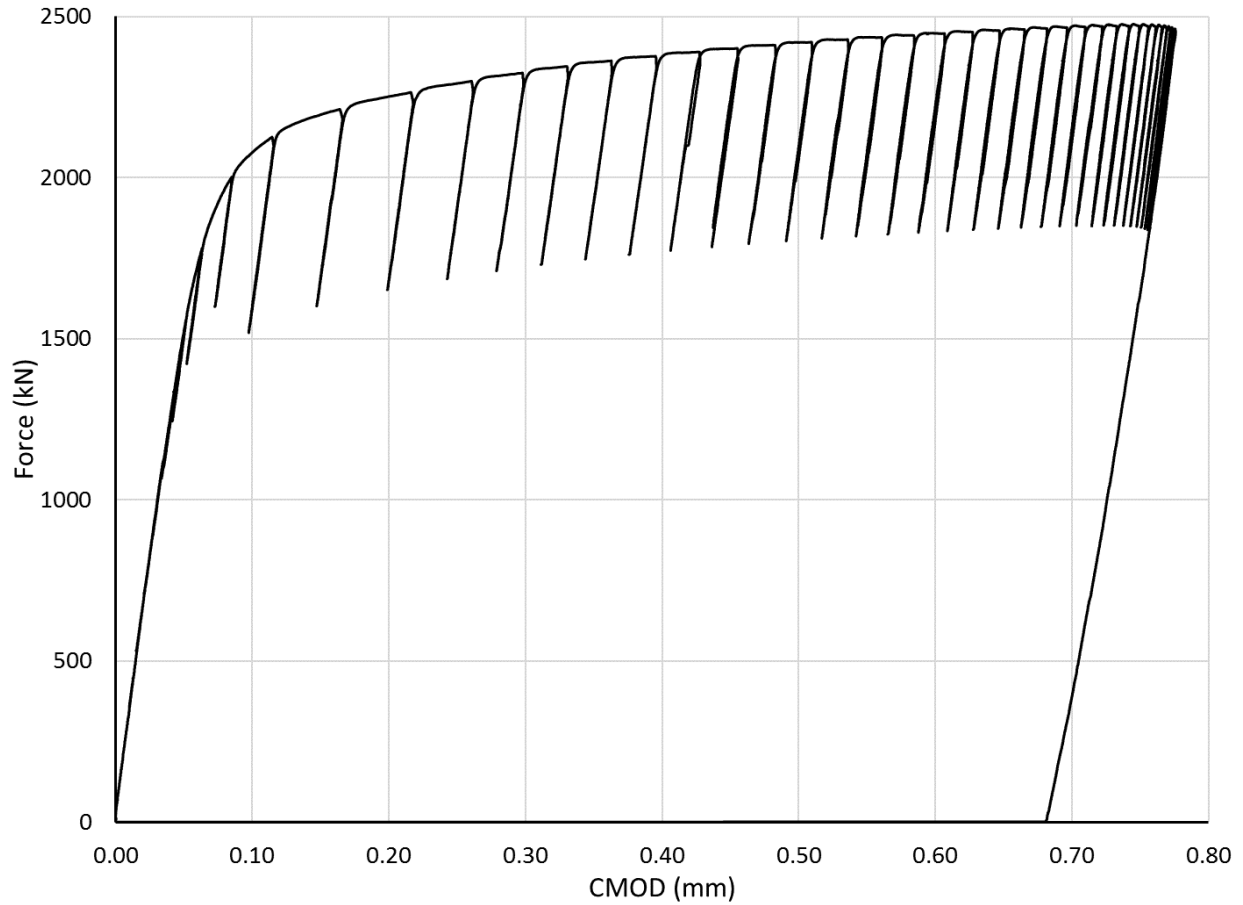


Figure C25 Plot of force vs. CMOD for 233 CWP-1. This plot shows the compressed unloading cycles at the end of the test which was a result of the net section necking and large increases in machine stroke with very little change in CMOD.

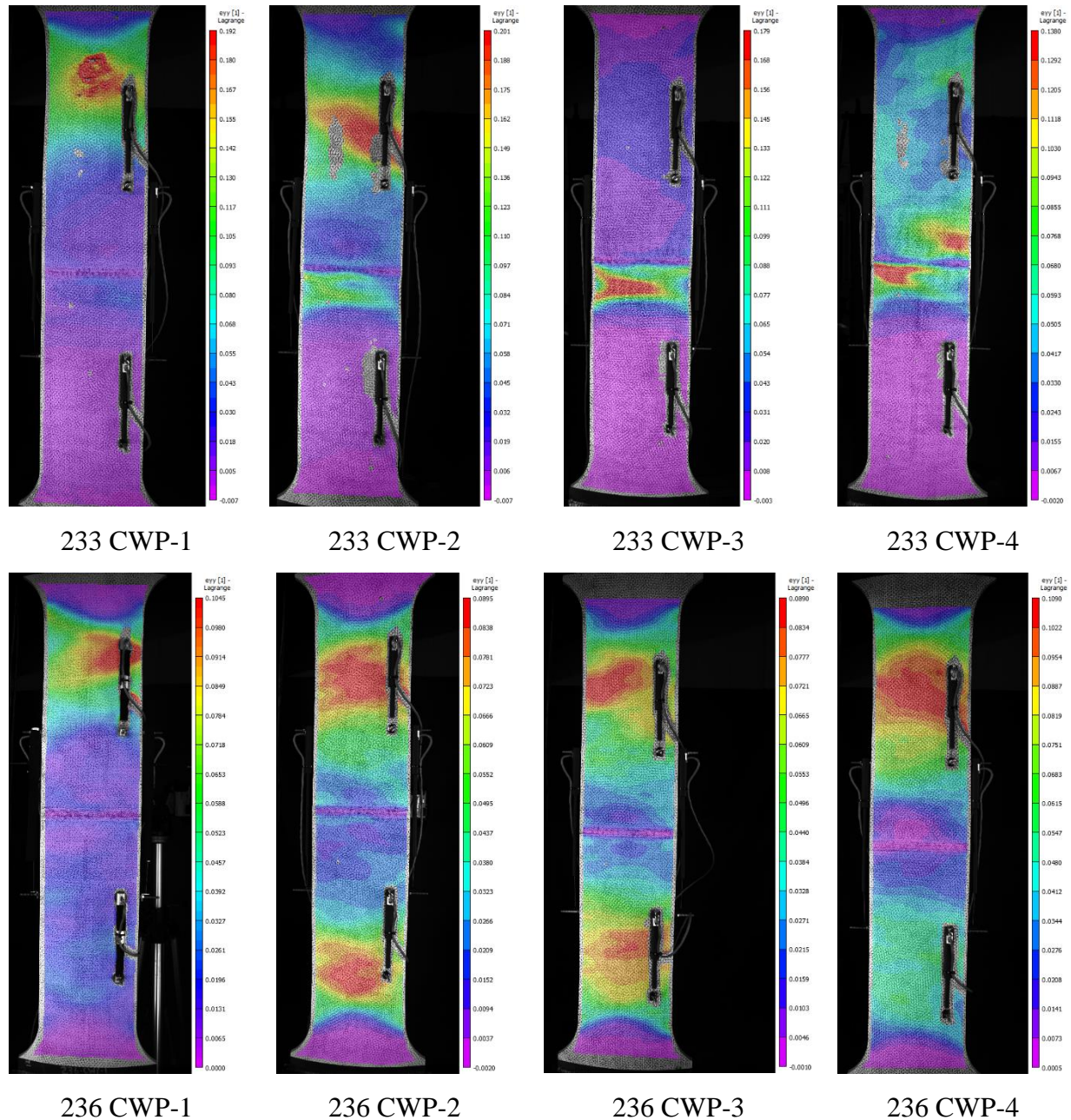


Figure C26 Processed DIC images for each CWP specimen at the end of each respective test. The images show the axial ϵ_{yy} (Lagrange) strain tensor distribution in the specimen. Color gradients are based on the maximum strain and are therefore not the same between specimens, however qualitative strain localizations are obvious.

C.8 Post-Test Surface Notch Mouth Opening Photographs

Each of the CWP specimens were plasma cut from the end-tabs and prepared for notch sectioning. Each of the CWP specimens were then saw cut to remove material adjacent the

notch. The sectioning plan is illustrated in Figure C27. Each of the notches were photographed and are presented in

Figure C28.

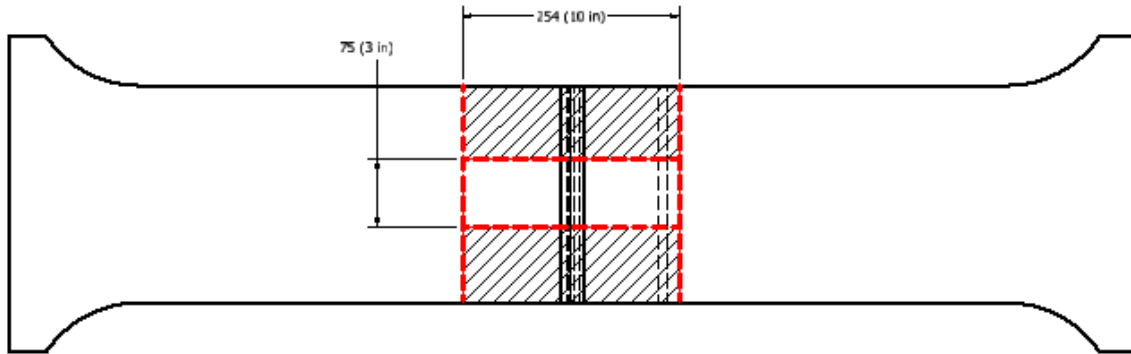


Figure C27 Illustration of the post-test sectioning plan. The end-tabs were cut from the specimens by use of plasma cutting and a band saw was used to further section the material adjacent the notch. A nominal 254 mm (10 in) by 75 mm (3 in) strip was retained. This view is of the 16 mm – 19 mm WT pipe (Weld 233 (Weld-2)) but the layout was identical for all specimens.

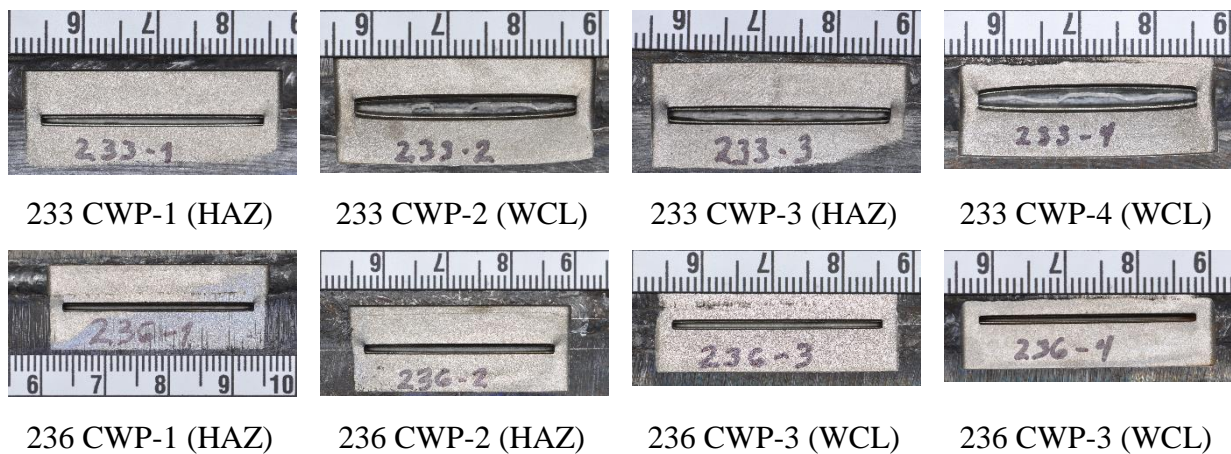


Figure C28 Post-test notch mouth opening photographs, scales shown are in units of cm

C.9 Post-Test Fracture Surface Photographs

The retained strips were heat tinted for approximately 45 mins at 300 °C and allowed to cool naturally back to room temperature. The retained strips from each specimen were cooled in

liquid nitrogen and the fracture surfaces were liberated by an overload in 4-pt bending. The fracture surfaces were then photographed and can be seen in Figure C29.



Figure C29 Post-test fracture surface photographs, scales shown are in units of cm